Journal of Colloid and Interface Science **210**, 8–17 (1999)
Article ID jcis.1998.5776, available online at http://www.idealibrary.com on IDEAL®

Aggregation Behavior of Tyloxapol, a Nonionic Surfactant Oligomer, in Aqueous Solution

Oren Regev* and Raoul Zana†,[1]

*Department of Chemical Engineering, Ben-Gurion University, 84105 Beersheva, Israel; and †Institut C. Sadron (CNRS), 6 rue Boussingault, 67000 Strasbourg, France

Received March 26, 1998; accepted July 29, 1998

The aggregation behavior of Tyloxapol, a nonionic surfactant oligomer with a repeating unit close to Triton X-100 (TX100), and a maximum degree of polymerization of about 7, has been investigated in aqueous solution by means of fluorescence probing, time-resolved fluorescence quenching (TRFQ) and transmission electron microscopy at cryogenic temperature (cryo-TEM). The plot of the pyrene fluorescence intensity ratio I_1/I_3 against the Tyloxapol concentration shows no clear evidence of a critical micelle concentration contrary to TX100. Nevertheless, the fitting of these data, assuming a partition of pyrene between Tyloxapol aggregates and water, yields cmc values in the micromolar range, i.e., about a hundred times lower than for the "monomer" TX100. The values of I_1/I_3 at high surfactant concentrations indicate that Tyloxapol micelles provide pyrene a less polar environment than TX100 micelles. The use of the viscosity-sensitive probe 1,3-dipyrenylpropane indicates that the microviscosity of Tyloxapol micelles is quite high, three to four times larger than that for TX100 micelles, and decreases rapidly with increasing temperature. Also the microviscosities of both TX100 and Tyloxapol micelles are larger than those for the micelles of the nonionic ethoxylated surfactant $C_{12}E_9$. The aggregation numbers of Tyloxapol and of TX100 micelles measured using TRFQ increase with temperature, with the Tyloxapol micelles being smaller than the TX100 micelles. Cryo-TEM shows that the Tyloxapol micelles remain spheroidal up to a concentration of about 10 wt%. At 15 wt%, some regions of ordered elongated micelles are also observed which may be the precursors of the hexagonal phase known to occur at about 35 wt%. © 1999 Academic Press

Key Words: **nonionic surfactant oligomer; Triton X-100; Tyloxapol; aggregation in aqueous solution; cmc; micelle shape; micelle microviscosity.**

INTRODUCTION

In recent years a new class of surfactants which can be broadly referred to as surfactant oligomers has attracted increasing interest (1–5). Surfactant oligomers are made up of two or more amphiphilic moieties connected at the level of, or very close to, the head groups by a spacer group. The surfactant dimers, also referred to as gemini surfactants (2), have been the most investigated. The interest in surfactant dimers and oligomers is due to the fact that they are characterized by much lower critical micelle concentration (cmc) values and much stronger surface tension lowering action than the corresponding conventional (monomeric) surfactants (1–5). These two properties determine most uses of surfactants in formulations. Surfactant trimers and tetramers are characterized by even lower cmc values than surfactant dimers (6–8). The work on surfactant dimers and oligomers has been recently reviewed (3–5). Thus far, the reported studies have essentially concerned cationic and anionic surfactant dimers. There has been no report on the properties of nonionic surfactant oligomers, probably because of difficulties in their synthesis. However, a nonionic surfactant oligomer, referred to as Tyloxapol, has been synthesized and described (9, 10) and can be obtained from chemical manufacturers. Tyloxapol is very close to being an oligomer of the much investigated Triton X-100 (TX100; see chemical structures in Scheme 1). The micelle formation by Tyloxapol and the phase diagrams of Tyloxapol/water and Tyloxapol/TX100/water mixtures have been investigated (11–13). In view of our current interest in surfactant oligomers and the availability of Tyloxapol we decided to investigate its aggregation behavior in aqueous solution and to compare it to that of its monomer, TX100. For this purpose we made use of fluorescence probing using the probes pyrene (cmc, micelle polarity) and 1,3-dipyrenylpropane (micelle microviscosity) (14–16). We also used time-resolved fluorescence quenching (micelle aggregation numbers) (17–20) and transmission electron microscopy at cryogenic temperature (direct imaging of the aggregates in the surfactant solutions) (21). The results reveal important differences between the properties of the micelles of Tyloxapol and TX100 and also between their aggregation behaviors.

EXPERIMENTAL

Materials

The sample of TX100 (Aldrich Chemicals, Europe) was used as received. A sample of Tyloxapol (Sigma) was extensively dialyzed against water using dialysis bags with a cutoff of about 1500 Da and the surfactant was recovered by extensive vacuum rotatory evaporation first under 15 mm mercury

[1] To whom correspondence should be addressed.

0021-9797/99 $30.00

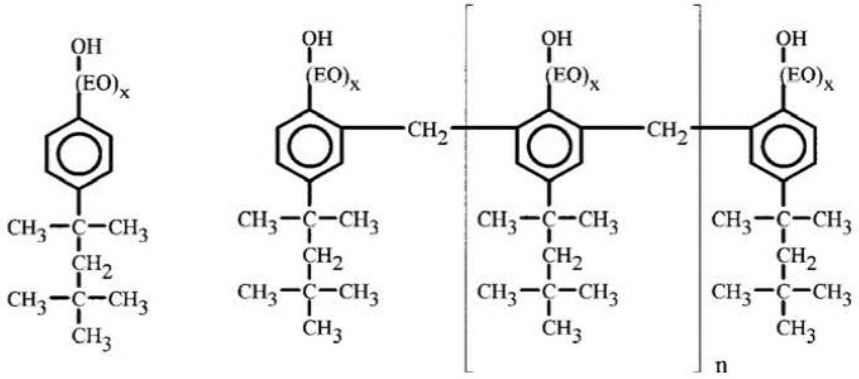

SCHEME 1. Chemical structures of Triton X-100 and of Tyloxapol (EO= $-CH_2CH_2O-$).

then under 1 mm mercury, at 40°C. The water content of the samples of raw and dialyzed Tyloxapol and of TX100 were measured using Karl–Fisher titration and found to be below 1 wt%. The concentrations given below have been corrected for that water content. The raw Tyloxapol was examined by size exclusion chromatography (solvent: tetrahydrofuran; four columns filled with beads of polystyrene cross-linked by divinylbenzene, of diameter 10 μm and of pore sizes 5, 10, 50, and 100 nm; detection: UV absorption or index of refraction). The chromatogram is shown in Fig. 1. Using the method reported in (22), this chromatogram was decomposed in a sum of four components corresponding to the monomer, dimer, trimer, and higher oligomers with percentages in weight of about 4.4, 10, 16.9, and 68.7, respectively (Fig. 1). The nonionic surfactant nonaethyleneglycol monododecyl ether ($C_{12}E_9$) was purchased from Fluka and used as received. The clouding temperatures of aqueous solutions of $C_{12}E_9$, TX100, and Tyloxapol at a concentration of 3 wt% were found to be 83 ± 0.5, 65.9 ± 0.2, and 90 ± 1°C, respectively.

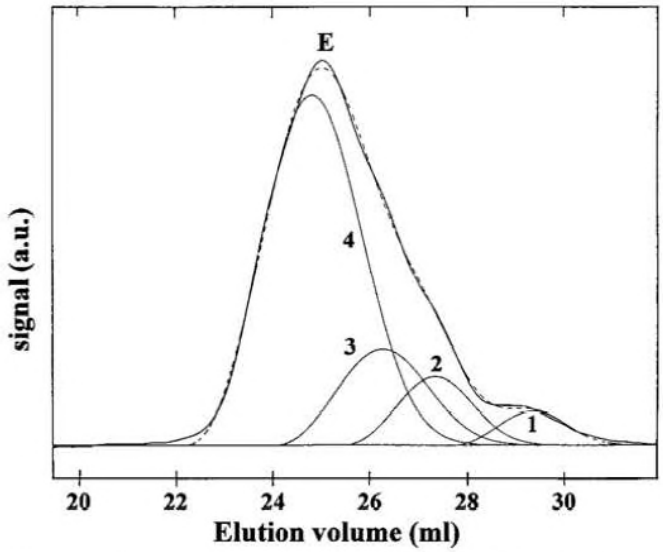

FIG. 1. Chromatogram of a 3 wt% solution of raw Tyloxapol in tetrahydrofuran. The signal (ordinate scale) is proportional to the refractive index of the eluted solution. The chromatogram has been analyzed according to the method in Ref. (22). Curve E is the experimental chromatogram. Curves 1, 2, 3, and 4 correspond to the monomer, dimer, trimer, and higher oligomer, respectively. The broken line curve is the sum of curves 1 to 4.

The fluorescence probes pyrene (purified by zone melting) and 1,3-dipyrenylpropane (DPP, from Molecular Probes, used without further purification) were the same as in previous studies (7). The quenchers of the pyrene fluorescence used for aggregation number determinations were dimethylbenzophenone (DMBP) (23) and tetradecylcyanopyridinium chloride (TCNPC) (24).

Water purifed using a Millipore Milli-RO 3Plus (resistance >18 mΩ) was used for the preparation of all solutions. The surfactant concentrations are expressed in wt% or in mol/L on the basis of molecular weights of 624 g/mol for TX100 and 636 g/mol for the repeating unit of Tyloxapol. These values assume an average of 9.5 ethoxy units per molecule or repeating unit (11–13).

Methods

Spectrofluorometry. The pyrene emission spectra were recorded using a Hitachi F4010 spectrofluorometer and used to obtain the ratio I_1/I_3 of the intensities of the first and third vibronic peaks in the emission spectra of pyrene solubilized in the micellar solutions. The excitation wavelength was set at 335 nm. For conventional surfactants the variation of I_1/I_3 with the surfactant concentration C permits one to obtain the cmc. In addition, the value of I_1/I_3 at $C \gg$ cmc gives a measure of the polarity sensed by pyrene at its micelle solubilization site (14, 15).

The emission spectra of DPP were recorded using the same spectrofluorometer in the range from 350 and 550 nm, using an excitation wavelength of 346 nm. These spectra showed an

emission due to the monomeric form of DPP in the range 360–400 nm with four vibronic peaks (I_M, intensity of the first peak located near 378 nm) and a broad emission maximum arising from the excimer form of DPP, centered at 485–490 nm (intensity I_E). The product of the intensity ratio I_M/I_E by fluorescence lifetime τ_E of the DPP excimer is proportional to the microviscosity of the surrounding medium (25, 26). The intensities I_M and I_E were measured using air-saturated solutions. The lifetimes in the same solutions were measured using a single photon counting apparatus (23, 24) at an excitation wavelength of 335 nm and monitoring the emission using a high-pass Kodak gelatin filter 4 ($\lambda > 460$ nm).

Time-resolved fluorescence quenching. We attempted to measure the aggregation numbers of Tyloxapol and TX100 micelles in aqueous solution using the time-resolved fluorescence quenching method (TRFQ) (15, 17–20) with pyrene as the fluorescent probe and DMBP or TCNPC as quenchers. The fluorescence decay curves were recorded using the same single photon counting apparatus which included a Type 7450 EGG-Ortec multichannel analyzer with a time base of 1024 channels (23, 24). As usual, the pyrene concentration was adjusted to be of about 1 to 2% of the micelle molar concentration, $[M]$, whereas the quencher molar concentration, $[Q]$, was adjusted to be close to $[M]$ (i.e., an average of one quencher per micelle). Prior to each experiment, the solutions investigated were deaerated by three successive freeze–pump–thaw cycles. The following fluorescence decay equations (17–20) were fitted to the experimental fluorescence decay curves of pyrene in the absence and in the presence of the quencher, respectively, using a weighted least-squares procedure (23, 24):

$$I(t) = I(0)\exp(-t/\tau) \quad [1]$$

$$I(t) = I(0)\exp\{-A_2t - A_3[1 - \exp(1 - A_4t)]\}. \quad [2]$$

In these equations $I(0)$ and $I(t)$ are the fluorescence intensities at time 0 and t, τ is the pyrene excited state lifetime in the absence of the quencher, and A_2, A_3, and A_4 are three fitting parameters. The micelle aggregation number, N, the rate constant for intramicellar quenching, k_Q, and the rate constant for probe and/or quencher exchange between micelles, k_e, may then be determined from

$$N = A_3\{(C - \text{cmc})/[Q]\}[1 + \epsilon]^2 \quad [3]$$

$$k_Q = A_4/[1 + \epsilon] \quad [4]$$

$$k_e = A_4 - k_Q = A_4\epsilon/(1 + \epsilon), \quad [5]$$

where C is the surfactant concentration in mole per dm^3 (15, 17–20), with

$$\epsilon = (A_2 - \tau^{-1})/A_3A_4. \quad [6]$$

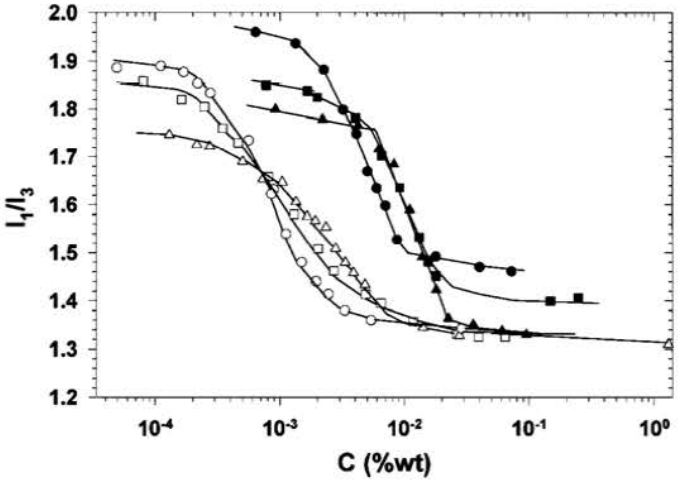

FIG. 2. Variations of I_1/I_3 with the surfactant concentration at 10°C (○, ●), 25°C (□, ■), and 40°C (△, ▲) for Tyloxapol (○, △, □) and TX100 (●, ▲, ■). The solid lines going through the data points are only guides to the eye.

The overall error on the aggregation number is estimated to be of ±10%.

Cryo-transmission electron microscopy (cryo-TEM). The specimens are prepared by blotting a 5-μl drop of the sample on a lacey carbon substrate (300 mesh, Ted Pella Inc.) in a controlled environment vitrification system (CEVS) (27), where temperature is controlled by a bulb and relative humidity is kept above 95% by a wet sponge to prevent sample evaporation. The specimen is blotted by a filter paper, resulting in the formation of a very thin sample film suspended over the grid, which is then vitrified very quickly in liquid ethane maintained at the liquid nitrogen temperature, 83 K (−190.15°C). The CEVS operation retains the original composition of the sample so that the original microstructures remain unaltered in the vitrified specimen. The vitrified specimen is then transferred by means of a Gatan cryoholder into a JEOL 1200EXII electron microscope operating at 100 kV in the conventional TEM mode with nominal underfocus of about 4 μm. The images are recorded at 83 K on SO-163 film. The low-dose mode of the electron beam is used to reduce radiation damage by the electron beam.

RESULTS AND DISCUSSION

The cmc and Micelle Micropolarity

Figure 2 shows the variations of the I_1/I_3 ratio with the surfactant concentration, C, for Tyloxapol and TX100 at 10, 25, and 40°C. The I_1/I_3 vs C plots for the raw and dialyzed samples of Tyloxapol were determined at 25°C and found to be coincident. This is not surprising in view of the very low fraction of monomer (4%) contained in the raw sample and which may be eliminated by dialysis. All of the measurements below refer to the raw sample. In all instances the intensity ratio shows a sigmoidal

decrease upon increasing C, revealing that pyrene goes from a hydrophilic to a hydrophobic environment. The latter is provided by surfactant aggregates when present in the solution with a sufficient volume fraction to solubilize pyrene. The two sets of results show important differences.

First, for Tyloxapol, the concentration range where most of the decrease of I_1/I_3 occurs is about 10-fold lower than that for TX100, showing that this surfactant oligomer provides pyrene with hydrophobic microdomains at a much lower concentration than its monomer. The cmc range of TX100 is seen to be around 0.01 wt%, i.e., 0.15 mM. The cmc of TX100 can be obtained using two approaches.

1. It is taken as the concentration corresponding to the intercept of the extrapolations of the high concentration part and of the rapidly varying part of the I_1/I_3 vs C plot (28). The cmc values are then found to be 0.012, 0.024, and 0.024 wt% which is about 0.19, 0.38, and 0.38 mM at 10, 25, and 40°C, respectively.

2. For several ionic and nonionic surfactants with the cmc in the 0.1 mM range the comparison of the electrical conductance or surface tension vs C plots and of the I_1/I_3 ratio vs C plots showed that the cmc, obtained for the conductance or surface tension plots (true cmc), closely corresponds to the concentration at the inflection point of the I_1/I_3 ratio vs C plot (29–31). This concentration is also very close to that at mid-decrease of the I_1/I_3 ratio. Using this procedure, the TX100 cmc values were found to be 0.05, 0.10, and 0.12 wt% (that is, 0.08, 0.16, and 0.19 mM) at 10, 25, and 40°C, respectively.

The cmc of TX100 has been reported to be between 0.25 and 0.27 mM at 25°C (32–34), a value between the ones given above at this temperature.

The second difference between Tyloxapol and TX100 is that the decrease of I_1/I_3 is much less steep for the former, stretching over nearly two decades of concentration for Tyloxapol against about one decade for TX100. In addition, there is no really sharp change at the end of the decrease for Tyloxapol, contrary to TX100. This complicates the determination of the "cmc" for Tyloxapol. Indeed, pyrene reports a partly hydrophobic environment already at a concentration of, say, 3×10^{-4} wt% (i.e., 5×10^{-6} M). However, the cmc, if it exists, may be located at an even lower concentration. Indeed at such a low amphiphile concentration the volume of the hydrophobic pseudo-phase is very small and a significant fraction of pyrene remains in the water, thereby reporting a partly aqueous environment even at concentrations above the cmc. The I_1/I_3 plots for Tyloxapol look very much like those characterizing systems with very low or zero cmc, where pyrene is progressively partitioned into hydrophobic aggregates, as the concentration of the amphiphile is increased (35). In such systems, the experimental fluorescence intensity ratio can be written in the form (35)

$$I_1/I_3 = (I_1/I_3)_{Ag} + [(I_1/I_3)_W - (I_1/I_3)_{Ag}]/[1 + K(C - \text{cmc})], \quad [7]$$

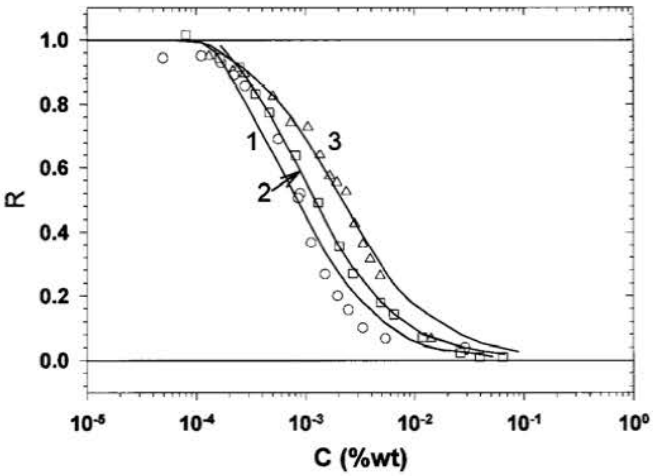

FIG. 3. Variations of the normalized fluorescence intensity ratio R with the surfactant concentration for Tyloxapol at 10°C (○), 25°C (□), and 40°C (△). The curves in solid lines 1, 2, and 3 have been calculated using Eq. [8] with the values K = 1434, 934, and 480 (wt%)$^{-1}$, and cmc = 1.1×10^{-4}, 1.4×10^{-4}, and 0.7×10^{-4} wt%, at 10, 25 and 40°C, respectively.

where $(I_1/I_3)_W$ and $(I_1/I_3)_{Ag}$ are the values of the intensity ratio in water and in the aggregate (that is, at $C \gg$ cmc), and K is an apparent binding constant of pyrene to the aggregates (K/55.5 is in fact the partition coefficient of pyrene between the hydrophobic domains considered as a pseudo-phase and water). The data in Fig. 2 have been normalized and replotted in Fig. 3 as R against C using a semi-logarithmic scale for the concentration, with R given by

$$R = [I_1/I_3 - (I_1/I_3)_{Ag}]/[(I_1/I_3)_W - (I_1/I_3)_{Ag}] = 1/[1 + K(C - \text{cmc})]. \quad [8]$$

The quantity R varies between 1 and 0 upon increasing C. It represents the fraction of pyrene solubilized in the aggregates. Its variation with log C is an S-shaped curve and $R = 0.5$ for $C - \text{cmc} = 1/K$. The R vs log C plots permit an easier comparison between surfactants of differing $(I_1/I_3)_{Ag}$ and also an easy visualization of the quality of the fit of Eq. [8] to the data. The plots 1–3 have been calculated using Eq. [8] with appropriate values of the binding constant and of the cmc given in the legend to Fig. 3. These plots are seen to provide a good fit for the Tyloxapol results at 25 and 40°C. The fit is somewhat less satisfactory at 10°C. The differences which may exist between the calculated curves and the data have been discussed and attributed to the large change of pyrene concentration in the aggregates at concentrations close to the cmc (35). The cmc values thus obtained are very inaccurate, around 10^{-4} wt%, which is 1.6 μM, at the three temperatures investigated. This value is very low, much lower than that for TX100. However, our results do not permit one to conclude whether the aggregates capable of binding pyrene in Tyloxapol solutions result from an aggregation of Tyloxapol around the pyrene mole-

cules, or reflect the solubilization or binding of pyrene to single Tyloxapol molecules which would be able to form intramolecular micelles, or arise from a true intermolecular association of Tyloxapol molecules as for normal amphiphiles at above the cmc. In the latter case our cmc value would be much smaller than that advanced by Westesen and Koch (12). Note that ionic surfactant oligomers have consistently been found to have much lower cmc values than the corresponding monomers. A similar behavior is expected for Tyloxapol with respect to TX100.

The third difference between TX100 and Tyloxapol is that at $C \gg$ cmc, as the temperature is decreased from 40 to 10°C, the value of I_1/I_3 increases from about 1.32 to 1.44 for TX100, but remains nearly constant at about 1.32 for Tyloxapol. At 25°C the values of I_1/I_3 are 1.32 and 1.4 for Tyloxapol and TX100, respectively, indicating that the micelles of Tyloxapol provide pyrene with an environment of lower polarity than TX100 micelles (14, 15). However, at 40°C, Tyloxapol and TX100 micelles are characterized by about the same value of I_1/I_3.

Microviscosity

The values of the DPP excimer lifetime and of the ratio I_M/I_E were determined for Tyloxapol and TX100 solutions at different concentrations and temperatures. We did not attempt to calculate absolute microviscosities from the results. Indeed this involves the use of a calibration plot (plot of $\tau_E I_M/I_E$ vs viscosity for a series of liquids of known viscosity) and the microviscosities thus obtained depend on the calibration curve used (36). Since we were essentially interested in comparing the micellar microviscosities of Tyloxapol and of its monomer TX100, all the results below concern the values of the product $\tau_E I_M/I_E$ which is referred to as microviscosity even though it is realized that it is only proportional to the microviscosity. At the outset it should be stated that the measurements of I_M/I_E for Tyloxapol solutions at temperatures below 40°C were difficult

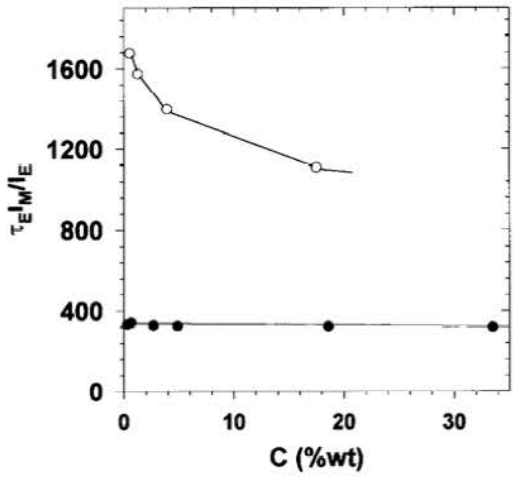

FIG. 4. Variations of the micelle microviscosity with the surfactant concentration for Tyloxapol (○) and TX100 (●) at 45°C.

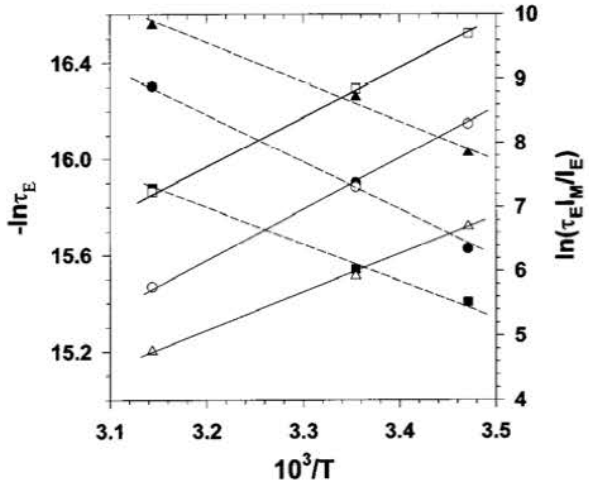

FIG. 5. Variations of the micelle microviscosity (solid lines) for Tyloxapol (□), TX100 (○), and $C_{12}E_9$ (△), and corresponding variations of the lifetime of the DPP excimer (broken lines) for Tyloxapol (■), TX100 (●), and $C_{12}E_9$ (▲), with temperature.

because of the extremely low values of the excimer intensity which reflect extremely large values of the microviscosity. The $\tau_E I_M/I_E$ values for Tyloxapol solutions below 40°C must be considered lower bound values.

Figures 4 and 5 show the variations of $\tau_E I_M/I_E$ with concentration and temperature (T), respectively, for Tyloxapol and TX100. In all instances the microviscosity of Tyloxapol aggregates is larger than that of TX100. A similar difference has been found between the microviscosity values of ionic surfactant oligomers and their corresponding monomers (7). Figure 4 shows that the microviscosity is nearly independent of the TX100 concentration but decreases somewhat as the Tyloxapol concentration is increased. Figure 5 shows that the microviscosity of both Tyloxapol and TX100 aggregates decreases steeply as the temperature increases. In the semi-logarithmic representation adopted in Fig. 5 ($\ln(\tau_E I_M/I_E)$ against $1/T$) the plots are linear; that is, one can write

$$\tau_E I_M/I_E = (\tau_E I_M/I_E)_0 \exp(-E_\eta^{\neq}/kT). \quad [9]$$

The slopes of the plots in Fig. 4 yield the values 61.2 and 62.2 kJ/mol for the activation energy $E_\eta^{\neq}$ of the microviscosity for TX100 and Tyloxapol micelles, respectively. Also represented in Fig. 5 are the semi-logarithmic variations of the lifetime τ_E of the DPP excimer with $1/T$. The plots are linear and yield the values 16.8 and 11.8 kJ/mol for the activation energy $E_{\tau E}^{\neq}$ of τ_E for TX100 and Tyloxapol.

For the sake of comparison we have also represented in Fig. 5 the variations of the values of τ_E and of the micellar microviscosity for the nonionic ethoxylated surfactant $C_{12}E_9$. It is seen that the microviscosity of $C_{12}E_9$ micelles is lower than that for TX100 and Tyloxapol micelles in the entire range of temperatures investigated. The activation energies for τ_E and

TABLE 1
Results of TRFQ Studies of Tyloxapol and TX100 Solutions

Surfactant	C (wt%)	T (°C)	Quencher	τ (ns)[a]	A_2^{-1} (ns)	A_3	$10^{-6} A_4$ (ns)	N[c]	$10^{-6} k_Q$ (s^{-1})	$10^{-5} k_e$ (s^{-1})
TX100	3.436	25	0.463 mM TCNPC	348.2 [241.1]	317.1	0.750	4.18	106	3.95	2.3
TX100	3.436	25	0.528 mM DMBP	348.2 [241.1]	310.2	0.850	4.78	104	4.40	3.8
TX100	3.436	40	0.528 mM DMBP	329.2 [191.0[b]]	268.4	1.176	4.57	155	4.07	5.0
Tyloxapol	3.418	25	0.570 M TPCNC	349.5 [281.0]						
Tyloxapol	3.456	40	0.590 mM DMBP	328.1 [225.4[b]]	285.6	0.427	3.88	63.8	3.04	8.4
Tyloxapol	3.418	40	0.570 mM TPCNC	328.1 [225.4[b]]	292.1	0.420	4.20	58.3	3.46	7.4
Tyloxapol[d]	3.35	55	1.236 mM TPCNC	[192.7]	152.8	1.68	4.22	99	3.52	7.2
$C_{12}E_9$	3.2	25	No quencher	345.6 [181.4]						
$C_{12}E_9$	3.2	40	No quencher	321.3 [135.8]						

[a] Values in brackets are for aerated solutions. The other values are for deaerated solutions.
[b] Values at 41°C.
[c] Values representing the number of surfactant hydrophobic moieties per micelle.
[d] This measurement has been performed on an air-saturated solution.

for the microviscosity for $C_{12}E_9$ are 13.7 and 49.8 kJ/mol, respectively.

Note that at a given temperature, the τ_E values increase in the order $C_{12}E_9$ < TX100 < Tyloxapol, that is, in the order of increasing microviscosity, in the temperature range investigated. The values of the pyrene fluorescence lifetimes in aerated micellar solutions of the three surfactants listed in Table 1 also increase in the order $C_{12}E_9$ < TX100 < Tyloxapol. However, Table 1 shows that identical values are found for the pyrene lifetime in deaerated micellar solutions, i.e., in the absence of solubilized oxygen, of the three surfactants. This fact confirms that the differences in DPP excimer and pyrene lifetimes found for the aerated solutions of the three surfactants are due to a loss of efficiency in the quenching of the probe fluorescence by molecular oxygen, which increases with the micelle microviscosity, as previously discussed (7).

The larger microviscosity of TX100 micelles with respect to micelles of ethoxylated nonionic surfactants C_mE_n (E = ethoxy group) explains why abnormally low values of the micelle aggregation number were measured in a previous time-resolved fluorescence quenching study of TX100 solutions (37). This study used the formation of excimer by pyrene (15). A later study (38) showed that the rate constant for intramicellar pyrene excimer formation is generally lower than the rate constant for pyrene quenching by alkylpyridinium ions. This fact together with the high microviscosity of TX100 resulted in decay plots where the linear part was not well developed. The fitting of Eq. [2] to the decay data yielded incorrect values of the fitting parameters and suggested a very rapid intermicellar exchange of pyrene. In turn, the analysis of the fitting parameters by means of Eqs. [2]–[5] yielded N values much lower than those obtained when using light scattering, for instance, particularly at low temperatures where the microviscosity of TX100 micelles is high.

The microviscosity of the mixtures of TX100 and Tyloxapol and the DPP excimer lifetime in these mixtures have been measured at 45°C. The results are represented in Fig. 6 against the Tyloxapol weight fraction. The continuous increases of τ_E and $\tau_E I_M/I_E$ between pure TX100 and Tyloxapol indicates the formation of mixed aggregates. This conclusion is supported by the results of Westesen *et al.* (13).

Aggregation Numbers

As discussed in the preceding paragraph the high microviscosity of TX100 and Tyloxapol micelles makes it necessary to use very efficient quenchers of pyrene fluorescence in order to make reliable estimates of the micelle aggregation numbers of these two surfactants. In a first attempt we used the tetradecylpyridinium ion as quencher. With both TX100 and Tyloxapol the decay plots were nearly linear and did not permit any meaningful determination of aggregation numbers. We there-

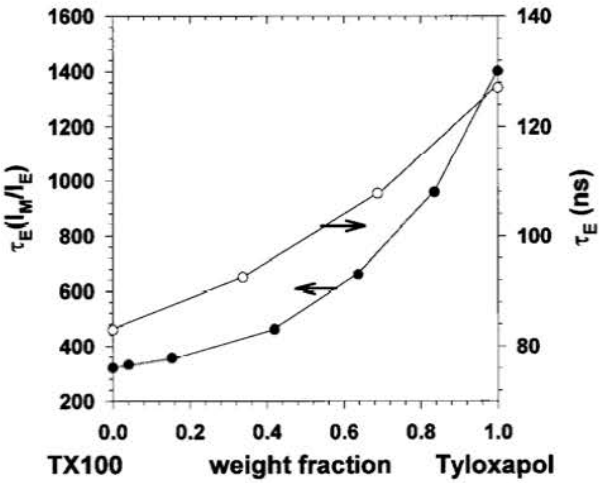

FIG. 6. Variations of the micelle microviscosity (●) and of the DPP excimer lifetime (○) for the TX100–Tyloxapol mixtures at 45°C, as a function of the Tyloxapol weight fraction in the mixture. Total surfactant concentration: about 5 wt%.

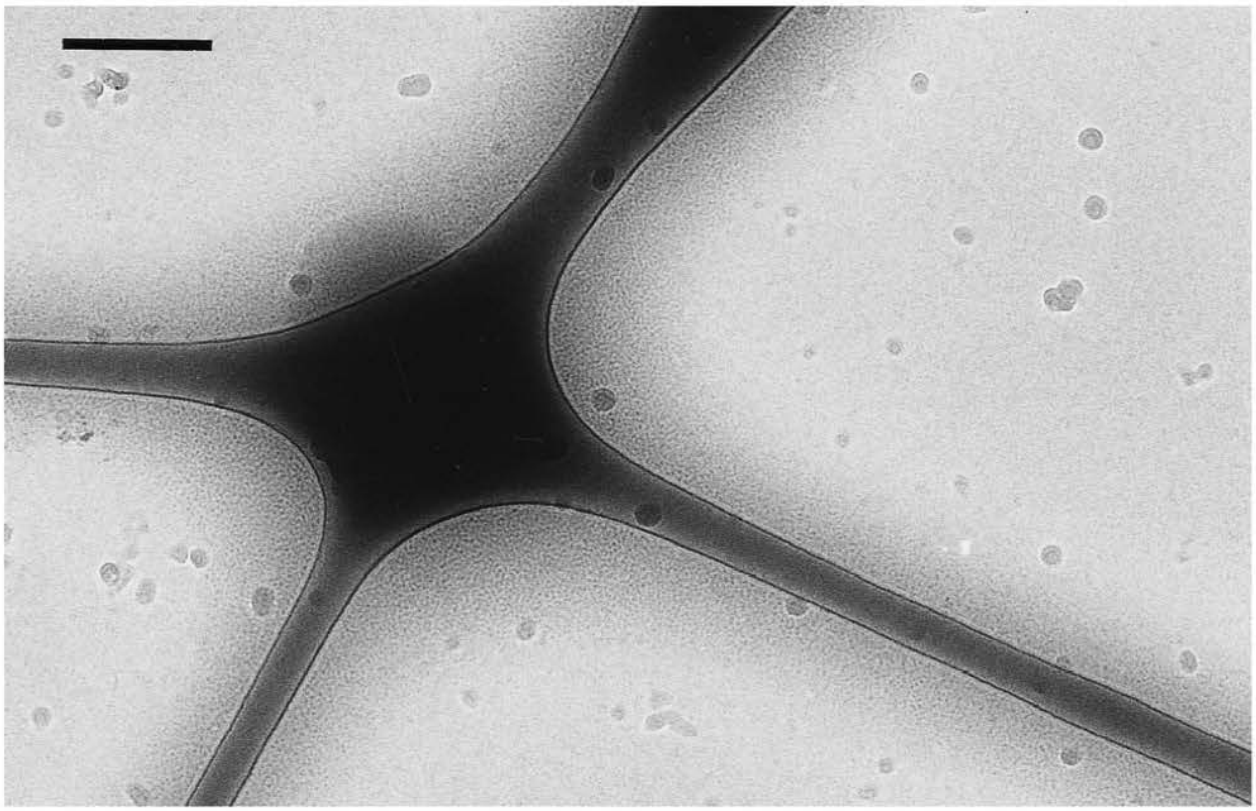

FIG. 7. Cryo-TEM micrograph of a 0.1 wt% Tyloxapol sample quenched from 25°C showing spheroidal micelles 5 nm in diameter. Dark objects are frost particles. Bar, 200 nm.

fore turned to the dimethylbenzophenone (23) and the tetradecylcyanopyridinium ion (24) which are very efficient quenchers of pyrene fluorescence. The results are summarized in Table 1. The surfactant concentration used was fairly high in order to ensure that the probe was nearly completely partitioned in the micelles.

The N values found for TX100 with the two quenchers at 25°C are identical within the experimental error. Also N increases much with temperature between 25 and 40°C, as for the nonionic surfactants C_mE_n (37–40). Our N values are in very good aggreement with those reported by Brown *et al.* (41), who used TRFQ with the pair pyrene–benzophenone. They also agree with the value reported in a recent dynamic light scattering study (42).

At 25°C the decay plots for Tyloxapol with the DMBP and TCNPC quenchers were close to linear and did not permit reliable estimates of aggregation number values. Recall that at this temperature the microviscosity of Tyloxapol micelles is still quite high and much larger than that of TX100. At 40 and 55°C, however, the decays were sufficiently curved to permit reliable estimates of N. The N values thus obtained (see Table 1) show that N increases with temprature as for TX100. However, the values for Tyloxapol are lower than those for TX100, indicating smaller micelles. This result is at variance with that found for ionic surfactant oligomers for which the micelle aggregation number, expressed as the number of alkyl chains per micelle, increased in going from the monomer to the dimer and trimer at a constant weight percent of surfactant (6, 43). However, Tyloxapol is an oligomer of larger oligomerization degree (up to seven) than those used so far. Also, as shown by the chromatogram in Fig. 1, the sample used is polydisperse. Mixed micellization most likely takes place between the various oligomers and may result in spherical micelles. Recall that the mixture of dodecyltrimethylammonium bromide (DTAB) which forms spherical micelles and of its dimer (denoted 12–2–12) which forms giant thread-like micelles yields spheroidal micelles at a relatively low mole fraction of DTAB (44).

The diameter of the hydrated Tyloxapol micelles has been calculated to be 6.3 nm, using an average value of 60 units for the aggregation number at 40°C, assuming a density of 1 for the aggregates (12), and an average hydration number of four water molecules per ethoxy group (45–49). A value of 7 nm was previously obtained (12) on the basis of distribution function analysis (50) of small angle X-ray scattering data for Tyloxapol micelles at a concentration of 3 wt%.

It is interesting to note that the values of the quenching rate constant, k_Q, for the Tyloxapol and TX100 micelles are fairly close at 40°C (see Table 1). This is so because k_Q is inversely proportional to the product of the microviscosity by the aggregation number (51–53). In the present case the higher micellar

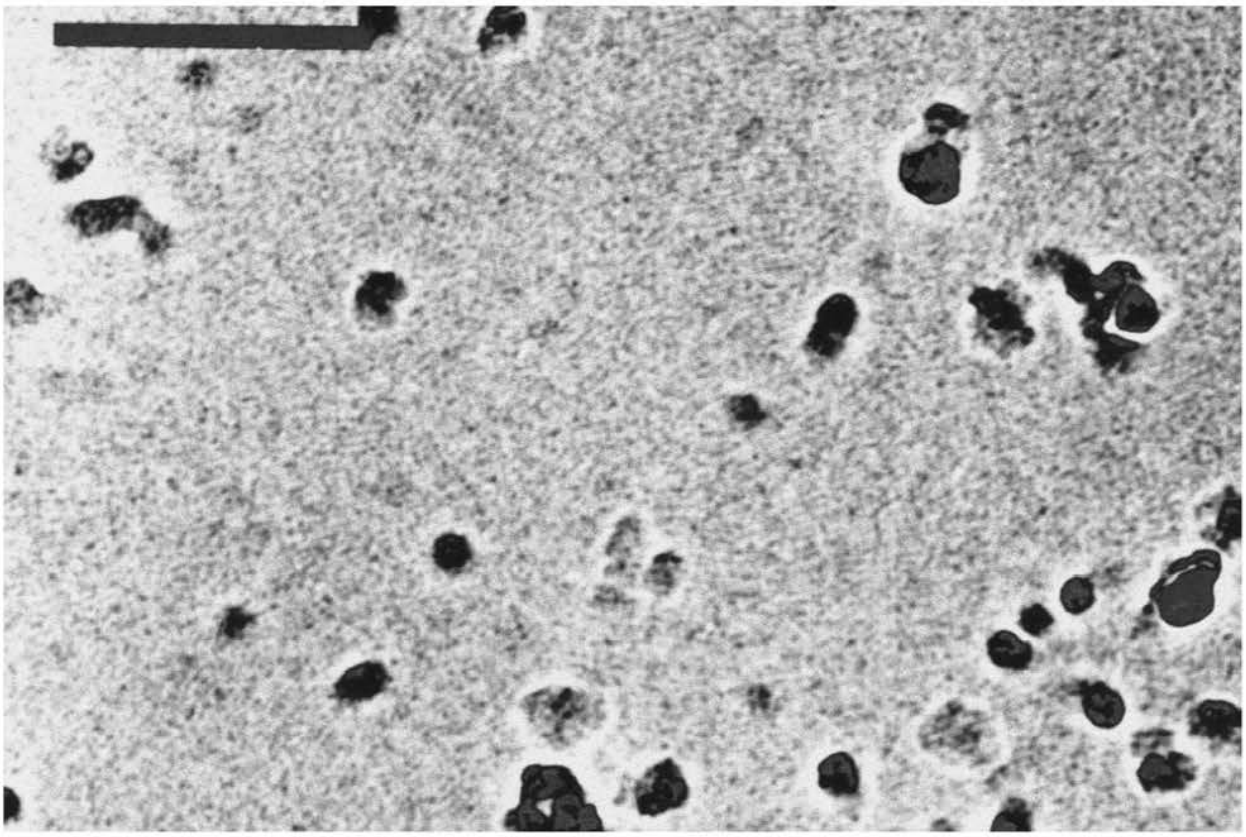

FIG. 8. Cryo-TEM micrograph of a 15 wt% Tyloxapol sample quenched from 25°C. Dark objects are frost particles. Bar, 200 nm.

microviscosity of Tyloxapol with respect to TX100 is largely compensated by the smaller micelle aggregation number of Tyloxapol with respect to TX100.

The values of the exchange rate constant are fairly low for both surfactants at 40°C. Exchange probably takes place through micelle collisions with temporary merging, as in micellar solutions of C_mE_n surfactants (37–40).

Microstructure of the Solutions (Cryo-TEM)

Cryo-TEM images of Tyloxapol at 0.1 wt% show spheroidal micelles 5 nm in diameter (Fig. 7). The diameter obtained confirms the preceding TRFQ results and also the small angle X-ray scattering (SAXS) results of Westesen and Koch (12). Note that in the cryo-TEM micrograph the micelles crowd in the thicker part of the vitrified film, close to the polymer support (21, 54, 55). Up to 10 wt% surfactant the micellar shape and size do not change much (not shown). However, at 15 wt%, still in the micellar phase, some regions of ordered elongated micelles are observed (Fig. 8). It is tempting to believe that these regions are precursors of the hexagonal phase, appearing only at 35 wt% (11, 12). Indeed, this result is in line with Westesen findings from the evolution of peaks in SAXS spectra with increasing surfactant concentration (12) mentioned as "strong interparticle interference between 10 to 35 wt% Tyloxapol." The *d* spacing calculated in this work (Fig. 2 of Ref. 12), 6 nm, is similar to the *d* spacing measured from our cryo-TEM image (Fig. 8).

Below 0.1 wt% we are unable to observe any form of aggregation in this system, most probably due to the low concentration of aggregates and/or their low aggregation number.

For the sake of comparison and also because the microstructure of solutions of TX100 has not yet been investigated by cryo-TEM, we have examined by this technique a 3 wt% solution of TX100 quenched from 25°C. The micrograph in Fig. 9 reveals spheroidal micelles with a diameter of about 5 nm, crowded in the thicker part of the film, close to the walls, similarly to Tyloxapol (Fig. 7). On the basis of the value 106 of the aggregation number of TX100 (Table 1), the TX100 micelles were expected to be elongated with an axial ratio of about 3.5 (56). Also the approximate value of the aggregation number of the micelles of a surfactant with an alkyl chain of effective carbon number 8.5, as TX100, and of volume 0.348 nm^3, close to that of a chain with 12 C atoms, such as TX100, is expected to be about 22. Thus for TX100, as for several other ethoxylated nonionic surfactants, the experimental micelle aggregation numbers are always larger than those for the corresponding minimum spherical micelles, and nevertheless the

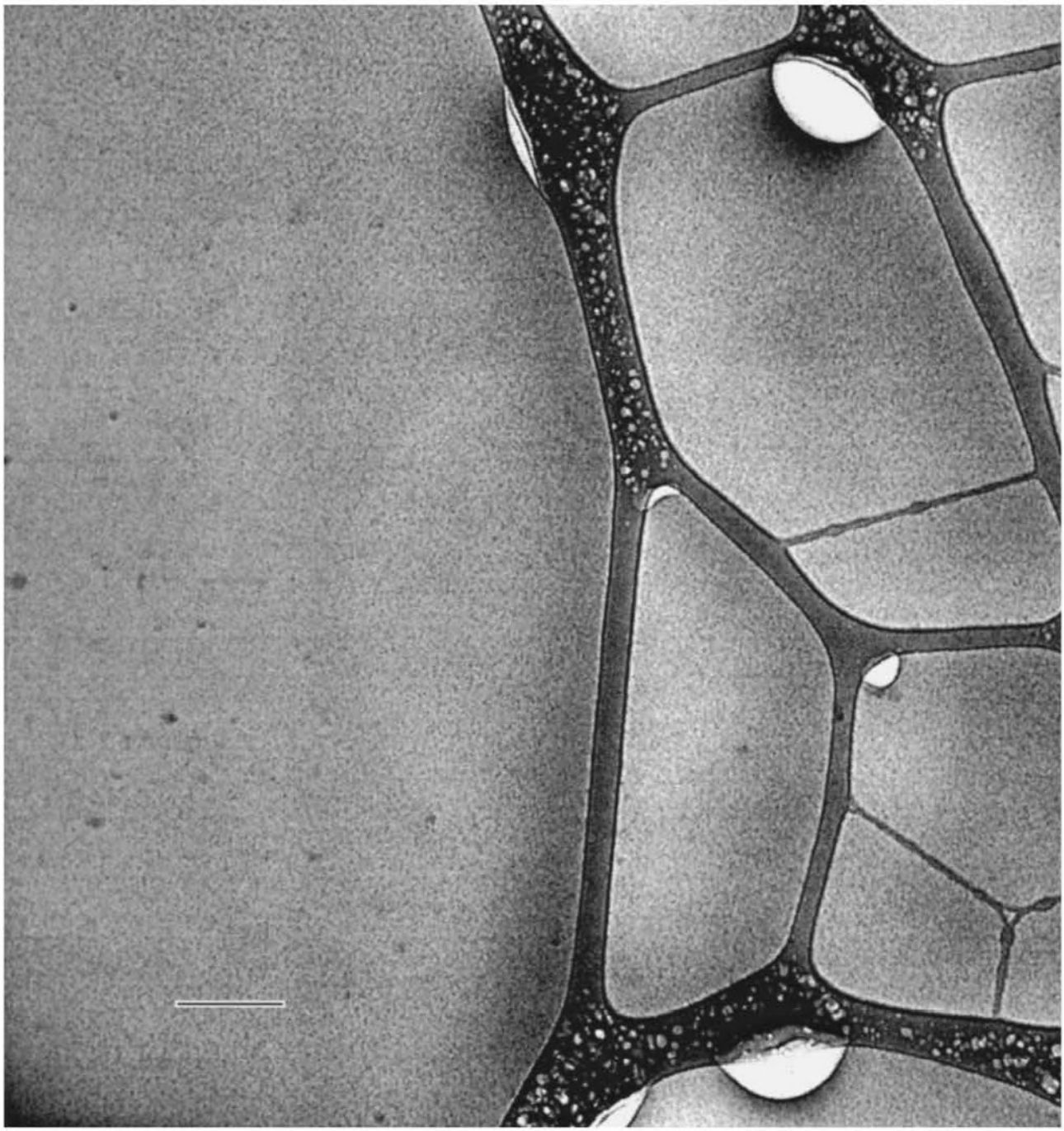

FIG. 9. Cryo-TEM micrograph of 3 wt% TX100 quenched from 25°C showing spheroidal micelles 5 nm in diameter. Dark objects are frost particles. Bar, 200 nm.

micelles are observed to be spheroidal by cryo-TEM (38–40). It has been advanced that the ethoxyleneoxide moieties may partially mix with the nonpolar groups (57, 58). If such is the case, spheroidal micelles, with much larger aggregation numbers than the minimum spherical micelle formed by a surfactant with the same alkyl chain, may be present in the solution as was recently discussed (40). The bulkiness of the head groups suggests another, possibly complementary, explanation. Indeed if one assumes that a uniform shell of polyethyleneoxide moieties covers the spherocylindrical micellar core of axial ratio 3.5 of the TX100 micelles, the thickness of this shell can be calculatd to be 0.332 nm. The axial ratio seen by cryo-TEM is that of the full micelles, core plus shell. Taking into account the shell, the axial ratio is then recalculated to be 1.65. Such a value is not large enough for the micelles to be seen as prolate particles.

CONCLUSIONS

The aggregation behavior of the nonionic surfactant oligomer Tyloxapol has been investigated and compared to that of its corresponding monomer, Triton X-100, in water. It has been found that aggregates that can shield pyrene from water are present in Tyloxapol solutions at a concentration about 100-fold lower than for TX100. However, the results did not permit us to exclude that Tyloxapol molecules can form intramolecular micelles or wrap around pyrene at a very low concentration, shielding it from water. The micropolarity provided by Tyloxapol micelles is lower than that of TX100 micelles at least at temperatures below 25°C whereas their microviscosity is about four times larger than that of TX100 micelles in the temperature range investigated. Finally, the micelles of Tyloxapol have been found to be smaller than those of TX100. This behavior is opposite to that found for ionic surfactant oligomers with respect to their corresponding monomers. Cryo-TEM showed spheroidal micelles in 3 wt% solutions of the two surfactants.

ACKNOWLEDGMENT

Thc authors thank Mr. A. Ramcau from thc Institut C. Sadron (Strasbourg) for determining the chromatogram of Tyloxapol shown in Fig. 1.

REFERENCES

1. Rosen, M., *Chem. Technol.* 30, (1993) and references therein.
2. Menger, F. M., and Littau, C. A., *Langmuir* **115,** 10083 (1993).
3. Zana, R., *Curr. Opin. Colloid Interface Sci.* **1,** 566 (1996), and references therein.
4. Zana, R., *in* "Specialist Surfactants" (I. Robb, Ed.), Chap. 4, p. 81. Chapman & Hall London, 1997, and references therein.
5. Zana, R., *in* "Structure–Performance Relationships in Surfactants" (K. Esumi and M. Ueno, Eds.), Chap. 6, p. 255. Dekker, New York, 1997, and references therein.
6. Zana, R., Lévy, H., Papoutsi, D., and Beinert, G., *Langmuir* **11,** 3694 (1995).
7. Zana, R., In, M., Lévy, H., and Duportail, G., *Langmuir* **13,** 5552 (1997).
8. In, M., and Zana, R., in preparation.
9. Lewis, A. J., "Modern Drug Encyclopedia," 16th ed. Yorke Medical Books, New York, 1981.
10. Sterling Organics, "Technical Bulletin on Tyloxapol."
11. Westesen, K., *Int. J. Pharm.* **102,** 91 (1994).
12. Westesen, K., and Koch, M. H. J., *Int. J. Pharm.* **103,** 225 (1994).
13. Westesen, K., Bunjes, H., and Koch, M. H. J., *J. Pharm. Sci.* **84,** 544 (1995).
14. Kalyanasundaram, K., and Thomas, J. K., *J. Am. Chem. Soc.* **99,** 2039 (1977).
15. Zana, R., *in* "Surfactant Solutions: New Methods of Investigation" (R. Zana, Ed.), Chap. 5, p. 241. Dekker, New York, 1987.
16. Zachariasse, K., *Chem. Phys. Lett.* **57,** 429 (1978).
17. Infelta, P., *Chem. Phys. Lett.* **61,** 88 (1979).
18. Tachiya, M., *Chem. Phys. Lett.* **33,** 289 (1975).
19. Almgren, M., *Adv. Colloid Interface Sci.* **41,** 9 (1992).
20. Gehlen, M., and De Schryver, F. C., *Chem. Rev.* **93,** 199 (1993).
21. Talmon, Y., *Ber. Bunsen-Ges. Phys. Chem.* **100,** 364 (1996).
22. Chaumont, P., and Merrill, E. W., *J. Chromatogr.* **303,** 177 (1984).
23. Anthony, O., and Zana, R., *Langmuir* **12,** 3590 (1996).
24. Alami, E., Van Os, N. M., Rupert, L. A. M., De Jong, B., Kerkhof, F. J. M., and Zana, R., *J. Colloid Interface Sci.* **160,** 205 (1993).
25. Turley, W. D., and Offen, H. W., *J. Phys. Chem.* **89,** 2933 (1985).
26. Miyagishi, S., Suzuki, H., and Asakawa, T., *Langmuir* **12,** 2900 (1996).
27. Bellare, J. R., Davis, H. T., Scriven, L. E., and Talmon, Y., *J. Electron. Microsc. Tech.* **10,** 87 (1988).
28. Frindi, M., Michels, B., and Zana, R., *J. Phys. Chem.* **95,** 4832 (1991); **96,** 8137 (1992).
29. Zana, R., Lévy, H., and Kwetkat, K., *J. Colloid Interface Sci.* **197,** 370 (1998).
30. Zana, R., and Lévy, H., *Colloids Surf. A: Physicochem. Eng. Asp.* **127,** 229 (1997).
31. Aoudia, M., and Zana, R., *J. Colloid Interface Sci.* **206,** 158 (1998).
32. Ross, S., and Olivier, J. R., *J. Phys. Chem.* **63,** 1671 (1959).
33. Ray, A., and Nemethy, G., *J. Phys. Chem.* **75,** 804 (1971).
34. Herrmann, C. U., and Kahlweit, M., *J. Phys. Chem.* **84,** 1536 (1980).
35. Anthony, O., and Zana, R., *Macromolecules* **27,** 3885 (1994).
36. Henderson, C. N., Selinger, B. K., and Watkins, A. R., *J. Photochem.* **16,** 215 (1981).
37. Zana, R., and Weill, C., *J. Phys. Lett.* **46,** L953 (1985).
38. Binana-Limbélé, W., and Zana, R., *J. Colloid Interface Sci.* **121,** 81 (1988).
39. Alami, E., Kamenka, N., Raharimihamina, A., and Zana, R., *J. Colloid Interface Sci.* **158,** 342 (1993).
40. Danino, D., Talmon, Y., and Zana, R., *J. Colloid Interface Sci.* **186,** 170 (1997).
41. Brown, W., Rymden, R., van Stam, J., Almgren, M., and Svensk, G., *J. Phys. Chem.* **93,** 2512 (1989).
42. Phillies, G. D., and Yambert, J. E., *Langmuir* **12,** 3431 (1996), and references therein.
43. Danino, D., Talmon, Y., and Zana, R., *Langmuir* **11,** 1448 (1995).
44. Zana, R., and Talmon, Y., *Nature* **362,** 228 (1993).
45. Paradies, H., *J. Phys. Chem.* **84,** 599 (1980).
46. Bratunets, A., Soboleva, N., Baran, A., and Tspko, M., *Ukr. Khim. Zh.* **49,** 37 (1983).
47. Nilsson, P. G., and Lindman, B., *J. Phys. Chem.* **87,** 4756 (1983).
48. Schefer, J., McDaniel, R., and Schoenhorn, B., *J. Phys. Chem.* **92,** 729 (1988).
49. Carlstrom, G., and Halle, B., *J. Chem. Soc. Faraday Trans. 1* **85,** 1049 (1989).
50. Glatter, O., *J. Appl. Crystallogr.* **10,** 415 (1977).
51. Lianos, P., Lang, J., Strazielle, C., and Zana, R., *J. Phys. Chem.* **89,** 1019 (1982).
52. Van der Auweraer, M., and De Schryver, F., *Chem. Phys.* **111,** 105 (1987).
53. Almgren, M., Alsins, J., Mukhtar, E., and van Stam, J., *J. Phys. Chem.* **92,** 4479 (1988).
54. Harwigsson, I., Söderman, O., and Regev, O., *Langmuir* **10,** 4731 (1994).
55. Regev, O., Ezrahi, S., Azerin, A., Wachtel, E., Garti, N., Kaler, E. W., Khan, A., and Talmon, Y., *Langmuir* **12,** 668 (1996).
56. The diameter and length of the cylinder of the micellar core were calculated to be 1.225 and 6.2 nm, on the basis of bond lengths, bond angles, and effective volume of the TX100 hydrophobic moiety: 0.348 nm^3. The axial ratio of the core is thus (6.2 + 2.45)/2.45 = 3.5.
57. Cooney, R., Barraclough, C., and Healey, T., *J. Phys. Chem.* **87,** 1868 (1983).
58. Robson, R. J., and Dennis, E. A., *J. Phys. Chem.* **81,** 1075 (1977).